Mn K-edge XAFS Studies of $La_{1-x}Sr_xMnO_3$: Local MnO_6 Structure as a Function of x

T. Shibata,[1] B. A. Bunker,[1] J. F. Mitchell[2]
[1]Department of Physics, University of Notre Dame, Notre Dame, IN, U.S.A.
[2]Materials Science Division, Argonne National Laboratory, Argonne, IL, U.S.A.

Introduction

There has been much more interest in the perovskite manganese (Mn) oxide since the rediscovery of the anomalous negative magnetoresistance that is called "colossal magnetoresistance" (CMR). These perovskite materials have the general formula $Ln_{1-x}R_xMnO_3$, where Ln is trivalent lanthanide earth and R is divalent alkaline earth. Doping produces the mixed valence states of Mn^{3+}/Mn^{4+}, which results in a rather complex structural, electronic, and magnetic phase diagram [1].

In the perovskite structures, the adjacent MnO_6 octahedra (six Mn-O bonds) are connected by sharing their corner oxygen atoms, forming a 3-D network. Since the electronic and magnetic interactions occur via Mn(3d)-O(2p)-Mn(3d) paths, the structures of these MnO_6 octahedra (bond lengths and Mn-O-Mn bond angle) represent a particularly important parameter with regard to understanding the physical properties of these perovskite materials. Because of the alloy structures and their intrinsically inhomogeneous nature, studies of the local structure are important. Two major methods are used to study local structure: (1) pair distribution function (PDF) analysis of the total neutron or x-ray scattering and (2) x-ray absorption fine structure (XAFS) spectroscopy. Because of the importance of the local structure, a number of works focus on the MnO_6 octahedral structures by using these methods.

$La_{1-x}Sr_xMnO_3$ (LSMO) is one of the canonical CMR materials. The MnO_6 octahedron of $LaMnO_3$ is subject to a Jahn-Teller (J-T) distortion with the cooperative rotation; as a result, the average structure is an orthorhombic structure. $LaMnO_3$ is an antiferromagnetic insulator with strong electronic correlation. Doping Sr continuously removes the distortion, and at an x of ~0.175 when x goes into a metallic phase, the (average) distortion is nearly completely removed and turns into a rhombohedral structure. The complete removal of the distortion in the metallic phase seems a natural consequence because of the more mobile electrons.

Louca et al. [2] studied neutron diffraction experiments and found by PDF analysis that the local structure is significantly different from the average structure. The local distortion exists up to $x = 0.35$ even in the metallic phase. Although the density of J-T polarons decreases linearly with x, the structure of the distorted MnO_6 essentially does not change with x (e.g., full J-T distortion remains). More recently, however, some reports in which similar methods are used [3] do not support Louca et al.'s results; thus, results seem to be inconclusive.

On the other hand, to the best of our knowledge, there are no XAFS works on LSMO materials. We therefore performed XAFS, the other local structural tool, at the Mn K edge at 10K and room temperature in order to examine the local MnO_6 structure as a function of x and to compare our results with the previous PDF results. We found some distortion does exist in the metallic phase as Louca et al. observed; however, the distortion is partially removed in the metallic phase. This is possibly a result of the increasing number of the double-exchange Mn^{3+}-Mn^{4+} pairs and the charge transferred partially between them. This is discussed with the localized polaron pictures.

Methods and Materials

The details of the sample preparation are described in Reference 4. We prepared various compositions for $0 \le x \le 0.475$ and $x = 1$ by two synthesis methods. The samples were ground and sieved through a 400-mesh (approximately 30-μm opening) and rubbed onto adhesive (Scotch™) tape. The tape samples were folded several times in order to have the necessary absorption lengths. We attached them to a cold finger of the Displex closed-cycle ^{4}He cryostat. Because of thermal conduction and radiation, the temperature might be slightly higher (by ~10K) for the low-temperature measurement, but it is still well below the T_N and T_C.

Transmission XAFS experiments were performed at the Materials Research Collaborative Access Team (MR-CAT) undulator beamline at the APS. The x-rays from the first harmonic of the undulator were monochromatized by a cryocooled Si(111) double-crystal monochromator, and a mirror was used for harmonic rejection. The gas-filled ion chambers were used to monitor the incident and transmitted photons.

XAFS oscillations, $\chi(k) = (\mu/\mu_0) - 1$, were extracted by using standard procedures [5]. Here μ, and μ_0 are the sample and (relatively smooth) atomic absorption coefficient, respectively. Since the La L_1-edge oscillations extended to the Mn K-edge region, we evaluated possible data overlap effects by fitting and confirmed that the problem is negligible. We also measured cubic $SrMnO_3$ (Pm3m, a = 3.80 Å, a known compound), and the spectra fit well to an average structure when the theoretical

calculation was used by the FEFF6 program [6]. Therefore, we used the scattering paths produced by FEFF6 to proceed with the analysis. The Fourier transform of $k^2\chi$, [χ(r)] is fit by using the FEFFIT program [7].

In this study, our interest mainly focuses on the first Mn-O bond; however, we include the higher neighbors to compensate for spectral leakage between the shells. The higher neighbors can be clearly seen for all the samples, indicating that the Mn ion environment is not distorted much, even for low doping samples. We performed fits of the Mn-O bonds in several different ways (e.g., a single bond length with a varied Debye-Waller factor [DWF, σ^2], and two bond lengths with a fixed DWF). We also attempted to fit so that the parameters are forced to be consistent with PDF results. When the bond length splitting (Δ) is small, Δ is correlated with the DWF and not resolved. In this case, we evaluated a possible distribution of the bond length. In addition, the population of the long bond (N_L) and the DWF is strongly correlated. We fixed N_L according to three models. Model A is a small polaron model ($N_L = 2 - 2x$) in which the number of distorted MnO_6 octahedra is proportional to the number of Mn^{3+} ions. Model B is a three-site polaron model ($N_L = 2$ to $6x$, x is <0.33) in which doped holes distribute to three Mn sites. Model C is a double-exchange model ($N_L = 2$ to $11x$, x is <0.175) in which the absence of distortion is assumed in the metallic phase. We compared the fit results among these three models.

Results and Discussion

Figure 1 shows χ(r) for various samples, where $k = 3$ to 14 $Å^{-1}$ is transformed. We plot the real part of the transform Re[χ(r)] because the phase information makes it easier to identify the contribution from oxygen. We also plot the amplitude for $SrMnO_3$ and $LaMnO_3$. The χ(r) is similar to the radial distribution function but appears at a smaller length than the actual atomic separation. For $SrMnO_3$, the peak at approximately 1.6 Å is from the Mn-O correlation's actual length of 1.9 Å. Because of the nondistorted structure, the peak appears sharp and large for $SrMnO_3$; however, for the other end compound $LaMnO_3$, the peak intensity is much smaller because of the distortion of the lattice. For $LaMnO_3$, we see an extra peak at 1.9 Å (marked L) coming from the long bond, plotted as a dashed line in Fig. 1. This can be fit by the Mn-O bond at 2.14 Å. The long bond feature, which appears as a positive peak in Re[χ(r)], is also seen for $x = 0.05$ and 0.075 samples. This feature becomes much smaller for $x = 0.175$, and at $x = 0.225$, this feature is not observed. This indicates that the distortion is significantly smaller and the length of the long bond goes within the resolution shown later.

Two lengths of 1.92 and 2.14 Å were observed for $LaMnO_3$. If we fix $N_L = 2$, the DWF of the short bond is $\sigma^2 = 0.0027$ $Å^2$, but the long bond has a large DWF as $\sigma^2 = 0.006$ $Å^2$, which corresponds to the ±0.06 Å (static) length distribution of the bond. The large length distribution can be interpreted as a variation of the distortion, leading to structural inhomogeneity.

For the alloy compounds of $x > 0$, we considered the three models described earlier, but for a short bond, the DWF and bond lengths are model independent. The short bond is nearly constant as 1.92 Å, with $\sigma^2 = 2.5$ to $\sim 3.0 \times 10^{-3}$ $Å^2$ for all x. For the very low doping region of $x < 0.075$, the structure is nearly model independent because of the small difference of N_L for small x. The local structure is similar to that of $LaMnO_3$ in terms of the bond lengths and the DWF for both the short and long bond. This may lead to the localization of the distortion or phase segregation features. This region shows similar Δ as PDF, although the absolute bond length is shifted.

For $0.075 \le x \le 0.1$, this region is model dependent. The small polaron model (Model A) gives a structure similar to that of the very small doping region. The DWF of the long bond has a value similar to that of $LaMnO_3$, although the bond length is slightly shorter as 2.08 Å. This model again would lead to a structural inhomogeneity, with variation of the distortion. The three-site polaron model (Model B) gives a much smaller DWF for the long bond and decreases from $x = 0.075$ to $x = 0.1$. The double-exchange model (Model C) gives zero DWF,

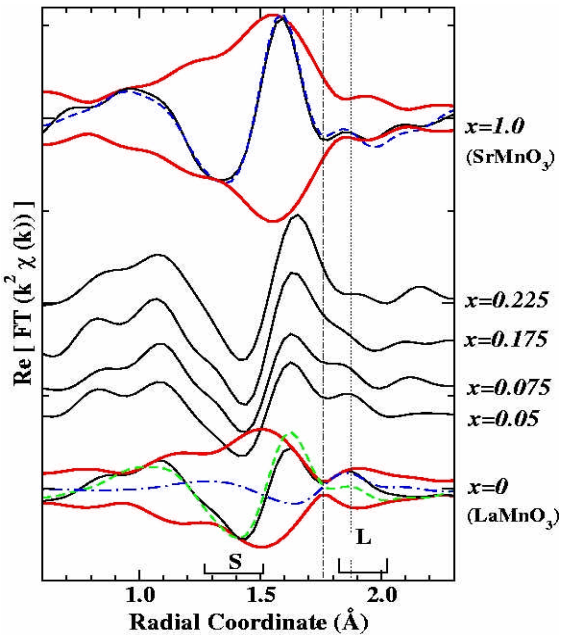

FIG. 1. Real part of the Fourier transform c(r) is shown for several samples. The amplitude is also shown for $SrMnO_3$ and $LaMnO_3$. The contribution from two different bond lengths is shown for $LaMnO_3$ (green and blue curve).

which should be excluded because of the physical meaning of DWF. From our data shown here, we cannot tell whether Model A or B is realized. Therefore, our data could support Louca et al.'s PDF results.

For x of >0.175, the possible splitting of the Mn-O peak is not resolved. For the x = 0.175 sample, for example, we could fit by a single bond length of 1.93 Å with σ^2 = 0.004 Å^2. If we evaluate the bond splitting by fixing the DWF as 0.0027 Å^2, when the thermal contribution is assumed, the long bond is 2.04 Å and Δ is ~0.1 Å. This is much smaller than the full J-T distortion of ~0.23 Å observed by PDF. We further determined uncertainties in Δ by fixing Δ to various values and allowing other parameters to vary. When we fix Δ to $\geq$ 0.15 Å, the fit is much worse (or gives large DWF); therefore, Δ is smaller than 0.15 Å. The upper values of Δ decrease with x when x is > 0.175, and Δ is again smaller than the full J-T distortion, indicating the partial removal of the distortion. Since for samples where x is <0.3, the peak height of the Mn-O bond in χ(r) is smaller than that of $SrMnO_3$ (not shown), it is possible that distortion remains in the metallic region. The partial removal of distortion seems to be a quite reasonable consequence because of the increasing number of Mn^{3+}-Mn^{4+} neighbors, where double-exchange interaction works. The partial charge transfer between these ions effectively reduced the distortion in these sites.

For the further doping level x of >0.375, the Mn-O bond has a single bond length with DWF similar to that of $SrMnO_3$, indicating the distortion has almost totally vanished. The fit results are shown in Fig. 2. When x is <0.175, the plot is based on Model B. The details of this work, including the room temperature analysis, will be published elsewhere [8].

In this report, we observed some local lattice distortion remains in the metallic region, but with increasing x in the metallic region, the distortion is partially removed, possibly as a result of the double-exchange interaction between Mn^{3+} and Mn^{4+} ions.

Acknowledgments

Use of the APS was supported by the U.S. Department of Energy (DOE), Office of Science, Office of Basic Energy Sciences, under Contract No. W-31-109-ENG-38.

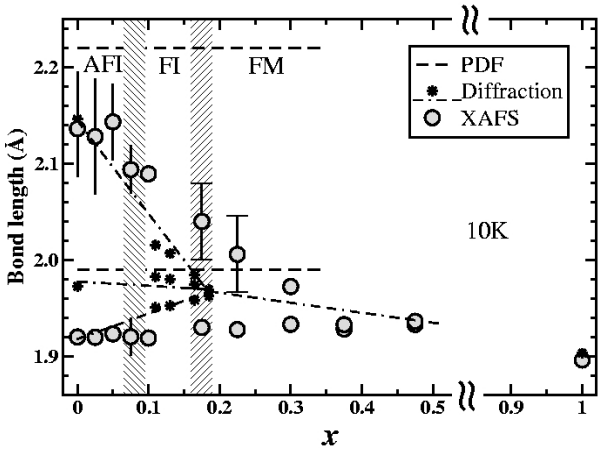

FIG. 2. Mn-O bond lengths as a function of x at 10K. Diffraction data [9] and PDF results are also shown. The vertical rise from the symbol for x < 0.1 is the possible bond length distribution deduced from DWF. Error bars for x = 0.175 and x = 0.225 are possible bond lengths (long bonds).

The MR-CAT is supported by DOE DE-FG02-94-ER45525 and member institutions. T. Shibata acknowledges the MR-CAT beamline scientists for their support at the experiments.

References

[1] See, for example, *Colossal Magnetoresisteive Oxide*, edited by Y. Tokura (Taylor & Francis, Inc., 2000).
[2] D. Louca et al., Phys. Rev. B **56**, R8475 (1997).
[3] Hibble et al., J. Phys. Condens. Matter **11**, 9221 (1999); Mellergård et al., ibid **12**, 4975 (2000).
[4] T. Shibata et al., Phys. Rev. Lett. (to be published in May 2002).
[5] *X-ray Absorption: Principles, Application, Techniques of XAFS, SEXAFS and XANES*, edited by R. Prince and D. C. Koningsberger (John Wiley & Sons, 1988).
[6] J. Rehr et al., Phys. Rev. Lett. **69**, 3397 (1992).
[7] M. Newville et al., Physica B **208** and **209**, 154 (1995).
[8] T. Shibata et al. (in preparation).
[9] B. Dabrowski et al., Phys. Rev. B **60**, 7006 (1999).